

FERMILAB-PUB 00/081-T

AMES-HET 00-02

April 2000

Determination of the pattern of neutrino masses at a Neutrino Factory

V. Barger¹, S. Geer², R. Raja², and K. Whisnant³

¹*Department of Physics, University of Wisconsin, Madison, WI 53706, USA*

²*Fermi National Accelerator Laboratory, P.O. Box 500, Batavia, IL 60510, USA*

³*Department of Physics and Astronomy, Iowa State University, Ames, IA 50011, USA*

Abstract

We study the precision to which the sign of δm_{32}^2 can be determined at a neutrino factory, as a function of stored energies and baselines. This is done by simultaneously fitting the channels $\nu_\mu \rightarrow \nu_\mu$, $\bar{\nu}_e \rightarrow \bar{\nu}_\mu$ from μ^- decays and the channels $\bar{\nu}_\mu \rightarrow \bar{\nu}_\mu$, $\nu_e \rightarrow \nu_\mu$ from μ^+ decays. We investigate the sensitivity reach in the parameter $\sin^2 2\theta_{13}$ to which one can determine the sign of δm_{32}^2 to 3 standard deviations as a function of the baseline length and magnitude of δm_{32}^2 with a 20 GeV muon storage ring. We find that for baselines longer than 2000 km, the sign of δm_{32}^2 can be determined for $\sin^2 2\theta_{13}$ down to the 10^{-3} level with 10^{20} decays of 20 GeV muons.

1 Introduction

The conceptual development of very intense muon sources [1] has led to a proposal [2] to use this new accelerator technology to build a Neutrino Factory in which an intense low energy muon beam is rapidly accelerated and injected into a storage ring with long straight sections. The muons decaying in these straight sections produce intense beams of highly collimated neutrinos. The technical and physics possibilities for building and using neutrino factories have been explored by many groups [3, 4]. The interest in neutrino factories is primarily driven by recent measurements from the SuperKamiokande (SuperK) collaboration [5], which indicate that muon neutrinos produced in atmospheric interactions of cosmic rays oscillate into other neutrino flavors, a result that is consistent with measurements made in other experiments [6]. The presence of a well-defined electron neutrino flux in the muon storage ring neutrino beams permits one to explore the effect of matter on the propagation of electron neutrinos. The analysis of the oscillation data leads to several scenarios of neutrino masses and mixing. In this paper, we investigate the effect of passage through matter on neutrino oscillations. We specifically consider the Large Angle MSW scenario (LAM) [7], which, as defined in the recent Fermilab six month physics study [8], has

$$\begin{aligned} |\delta m_{32}^2| &= 3.5 \times 10^{-3} \text{eV}^2, & |\delta m_{21}^2| &= 5 \times 10^{-5} \text{eV}^2, \\ \sin^2 2\theta_{23} &= 1.0, & \sin^2 2\theta_{12} &= 0.8, & \sin^2 2\theta_{13} &= 0.04 \end{aligned} \quad (1)$$

and the CP violating phase $\delta = 0$. However, to the extent that the contributions from the subleading solar δm_{21}^2 scale are small, our results apply approximately to our solar scenarios. The transition probabilities in the leading oscillation approximation for propagation through matter of constant density are [9, 10, 11, 12]

$$\begin{aligned} P(\nu_e \rightarrow \nu_\mu) &= s_{23}^2 \sin^2 2\theta_{13}^m \sin^2 \Delta_{32}^m, \\ P(\nu_e \rightarrow \nu_\tau) &= c_{23}^2 \sin^2 2\theta_{13}^m \sin^2 \Delta_{32}^m, \\ P(\nu_\mu \rightarrow \nu_\tau) &= \sin^2 2\theta_{23} \left[(\sin \theta_{13}^m)^2 \sin^2 \Delta_{21}^m + (\cos \theta_{13}^m)^2 \sin^2 \Delta_{31}^m - (\sin \theta_{13}^m \cos \theta_{13}^m)^2 \sin^2 \Delta_{32}^m \right]. \end{aligned} \quad (2)$$

The oscillation arguments are given by

$$\Delta_{32}^m = \Delta_0 S, \quad \Delta_{31}^m = \Delta_0 \frac{1}{2} \left[1 + \frac{A}{\delta m_{32}^2} + S \right], \quad \Delta_{21}^m = \Delta_0 \frac{1}{2} \left[1 + \frac{A}{\delta m_{32}^2} - S \right], \quad (3)$$

where S is given by

$$S \equiv \sqrt{\left(\frac{A}{\delta m_{32}^2} - \cos 2\theta_{13} \right)^2 + \sin^2 2\theta_{13}}, \quad (4)$$

and

$$\Delta_0 = \frac{\delta m_{32}^2 L}{4E} = 1.267 \frac{\delta m_{32}^2 (\text{eV}^2) L (\text{km})}{E_\nu (\text{GeV})}. \quad (5)$$

$$\sin^2 2\theta_{13}^m = \frac{\sin^2 2\theta_{13}}{\left(\frac{A}{\delta m_{32}^2} - \cos 2\theta_{13} \right)^2 + \sin^2 2\theta_{13}}. \quad (6)$$

The amplitude A for $\nu_e e$ forward scattering in matter is given by

$$A = 2\sqrt{2}G_F N_e E_\nu = 1.52 \times 10^{-4} \text{ eV}^2 Y_e \rho(\text{ g/cm}^3) E(\text{ GeV}). \quad (7)$$

Here Y_e is the electron fraction and $\rho(x)$ is the matter density. For neutrino trajectories that pass through the earth's crust, the average density is typically of order 3 gm/cm^3 and $Y_e \simeq 0.5$. The oscillation probability $P(\nu_e \rightarrow \nu_\mu)$ is directly proportional to $\sin^2 2\theta_{13}^m$, which is approximately proportional to $\sin^2 2\theta_{13}$. There is a resonant enhancement for

$$\cos 2\theta_{13} = \frac{A}{\delta m_{32}^2}. \quad (8)$$

For electron neutrinos, A is positive and the resonance enhancement occurs for positive values of δm_{32}^2 . The reverse is true for electron anti-neutrinos and the enhancement occurs for negative values of δm_{32}^2 . Thus for a neutrino factory operating with positive stored muons (producing a ν_e beam) one expects an enhanced production of opposite sign (μ^-) charged-current events as a result of the oscillation $\nu_e \rightarrow \nu_\mu$ if δm_{32}^2 is positive and vice versa for stored negative beams [9, 12, 13, 14, 15].

This enhancement is evident in Fig. 1, which shows the ratio of $\bar{\nu}_e \rightarrow \bar{\nu}_\mu$ events from μ^- decays to $\nu_e \rightarrow \nu_\mu$ events from μ^+ decays for 20 GeV muons and a 50 kt detector, assuming the oscillation parameters of Eq. (1). The results for two other values of δm_{32}^2 are also presented in Fig. 1. This figure shows that for larger L the ratio of wrong-sign muon events is sensitive to the sign of δm_{32}^2 .

The magnitude of δm_{32}^2 is determined from the disappearance of muon neutrinos due to the oscillation $\nu_\mu \rightarrow \nu_\tau$, since it can be shown that for the baselines under consideration here, the matter effects are small in this channel (see Fig. 2, curves 2 and 3 of Ref. [9]). The oscillation probability $P(\nu_\mu \rightarrow \nu_\tau)$ can thus be approximated by $\cos^4 \theta_{13} \sin^2 2\theta_{23} \sin^2(\Delta_0)$ as though it were in vacuum for baselines as far as 4000 km. (See the section ‘‘Method’’ for a correction to this approximation for matter effects for longer baselines.)

2 Method

In order to extract both the sign and magnitude of δm_{32}^2 , we simultaneously four channels (i) $\nu_\mu \rightarrow \nu_\mu$ (ii) $\bar{\nu}_e \rightarrow \bar{\nu}_\mu$ (iii) $\bar{\nu}_\mu \rightarrow \bar{\nu}_\mu$ (iv) $\nu_e \rightarrow \nu_\mu$. The first two channels are measured when $N \mu^-$ decays occur in the storage ring and the second two channels are observed when $N \mu^+$ decays occur [16].

We study the extraction of oscillation parameters in two scenarios:

- A muon storage ring with $N = 10^{20}$ muon decays and a 50 kiloton detector.
- A muon storage ring with $N = 10^{19}$ muon decays and a 50 kiloton detector. A 20 GeV version of this is known as an ‘‘entry level’’ neutrino factory.

Our study is performed for baselines ranging from 732 km up to 7332 km and stored muon energies ranging from 20 GeV to 50 GeV. We calculate the neutrino event rates by propagating the neutrinos through matter, taking into account the variations in the density profile using the Preliminary Reference Earth Model [17] by solving the evolution equations

numerically. Realistic detector resolutions are used that are appropriate for a magnetized iron scintillator detector. We assume a muon energy resolution $\frac{\sigma}{E_\mu} = 0.05$ and a hadronic shower resolution of $\frac{\sigma}{E_h} = 0.53/\sqrt{E_h}$ for showers of energy $E_h > 3$ GeV and $0.8/\sqrt{E_h}$ for showers of energy $E_h < 3$ GeV. We accept only events that possess muons of true energy greater than 4 GeV. Figure 2 shows the wrong-sign muon appearance spectra with these cuts as function of δm_{32}^2 for both μ^+ and μ^- beams for both signs of δm_{32}^2 at a baseline of 2800 km. The resonance enhancement in wrong sign muon production is clearly seen in Fig. 2 (b) and (c). Using these histograms and similar ones for the disappearance channels, it is possible to predict the spectrum in any channel for any value of δm_{32}^2 in the range of interest by polynomial interpolation of the histograms bin by bin with the method of divided differences. For the interpolation, the disappearance probabilities can be treated to first order as though they are due to vacuum oscillations (i.e. matter effects can be neglected) and are proportional to $\cos^4 \theta_{13} \sin^2 2\theta_{23}$. For the longer baselines, the matter effects affect these disappearance rates slightly, as can be seen from Fig. 3 of Ref. [9]. The difference in the disappearance rates for positive and negative δm_{32}^2 is proportional to $\sin^2 2\theta_{13}$, vanishing as $\sin^2 2\theta_{13} \rightarrow 0$. For the channel $\nu_\mu \rightarrow \nu_\mu$, the positive δm_{32}^2 solution approaches the negative δm_{32}^2 solution as $\sin^2 2\theta_{13} \rightarrow 0$, the reverse being the case for anti-neutrinos. We use this behavior to interpolate the disappearance spectra as a function of $\sin^2 2\theta_{13}$. The event rates in both the appearance and disappearance channels depend only on the three vacuum parameters $\sin^2 2\theta_{23}$, $\sin^2 2\theta_{13}$, and δm_{32}^2 . Using this interpolation scheme, we can generate events for any combination of these parameters for various muon momenta and baselines. Most of the information on the sign of δm_{32}^2 comes from the appearance channels and the precision on the magnitude of δm_{32}^2 comes from the disappearance channels [9, 12, 14].

2.1 Backgrounds

The background for the wrong-sign muon appearance channels arise from three sources: (i) charm production, (ii) π, K decay events producing wrong sign muons in neutral current interactions, and (iii) π, K decay events producing wrong sign muons in charged-current (CC) events where the primary muon was considered lost [8]. A more detailed study of the backgrounds [8] has shown that significant reductions are obtained by demanding that $P_t^2 > 2 \text{ GeV}^2$, where P_t^2 is defined as the transverse-momentum-squared of the muon with respect to the hadronic shower direction. Imposing this cut results in a further signal efficiency of 0.9 [18] for the CC disappearance channels, 0.62 for the μ^+ beam appearance signal and 0.45 for the μ^- beam appearance signal. This results in an average background/disappearance CC signal rate of 0.45×10^{-4} for μ^+ beam appearance channel and 0.25×10^{-5} for the μ^- beam appearance channel. The difference in these rates between the μ^+ and μ^- beams is due to the different kinematical distributions of the neutrino and anti-neutrino CC interactions. We fold these rates into the theoretical prediction for each channel. We also assume a normalization systematic uncertainty of 1% between the μ^+ beam and μ^- beam events.

Table 1 shows the wrong sign muon appearance event rates and background rates for an “entry level” machine which shows appreciable rates for events in the appearance channels and backgrounds that are negligible for baselines of 2800 km or higher.

2.2 Fitting

The events are generated in the 4 channels $\nu_\mu \rightarrow \nu_\mu$, $\bar{\nu}_e \rightarrow \bar{\nu}_\mu$, $\bar{\nu}_\mu \rightarrow \bar{\nu}_\mu$, and $\nu_e \rightarrow \nu_\mu$, for both signs of δm_{32}^2 . They are subjected to simultaneous fits for the three parameters $\sin^2 2\theta_{13}$, $\sin^2 2\theta_{23}$, and δm_{32}^2 , with δm_{32}^2 alternately constrained to have the same sign and opposite sign as the generated events [19]. The difference in negative log-likelihood, ΔL , between the fits with the sign of δm_{32}^2 being constrained to be the same as and opposite to the input sign, is evaluated for a number of fits for a particular value of $\sin^2 2\theta_{13}$. This is repeated for a range of $\sin^2 2\theta_{13}$. It is empirically found that the average ΔL varies linearly with $\sin^2 2\theta_{13}$ and this is used to estimate that value of $\sin^2 2\theta_{13}$ at which $\Delta L=4.5$, i.e a Gaussian 3σ ability to differentiate the sign of δm_{32}^2 . This value of $\sin^2 2\theta_{13}$ we define as the 3σ reach of $\sin^2 2\theta_{13}$. We only fit for the number of events and not the shape of the spectra, since at the 3σ point statistics are such that shape information contributes little.

Table 1: Wrong-sign muon rates for a 50 kt detector (with a muon threshold of 4 GeV) a distance L downstream of a muon factory (energy E_μ) providing 10^{19} muon decays. Rates are shown for LAM scenario of Eq. (1) with both signs of δm_{32}^2 considered separately. The background rates listed are for each sign of δm_{32}^2 and do not depend on the sign of δm_{32}^2 .

E_μ GeV	L km	μ^+ stored			μ^- stored		
		$\delta m_{32}^2 > 0$	$\delta m_{32}^2 < 0$	Backg	$\delta m_{32}^2 > 0$	$\delta m_{32}^2 < 0$	Backg
20	732	32.5	22.7	9.6	14.3	11.6	0.9
20	2800	28.7	5.7	0.3	3.2	11.7	0.0
20	7332	20.4	0.6	0.0	0.2	8.5	0.0
30	732	54.5	38.5	19.1	23.0	18.3	1.9
30	2800	49.2	13.1	0.8	7.4	18.4	0.1
30	7332	26.2	1.7	0.0	0.7	11.9	0.0
40	732	56.7	40.2	17.7	23.6	18.7	1.7
40	2800	51.3	14.7	0.8	8.2	18.7	0.1
40	7332	26.8	1.9	0.0	0.8	11.3	0.0
50	732	53.3	37.9	15.7	21.9	17.3	1.5
50	2800	47.7	13.9	0.7	7.9	17.4	0.1
50	7332	25.8	1.9	0.0	0.8	10.8	0.0

3 Results

Figure 3 shows the difference in negative log-likelihood between a correct and wrong-sign mass hypothesis expressed as a number of equivalent Gaussian standard deviations versus baseline length for muon storage ring energies of 20, 30, 40 and 50 GeV. The values of the oscillation parameters are for the LAM scenario in Eq. 1. Figure 3(a) is for 10^{20} decays for each sign of stored energy and a 50 kiloton detector and positive δm_{32}^2 (b) for negative δm_{32}^2 for various values of stored muon energy. Figures 3 (c) and (d) show the corresponding curves for 10^{19} decays and a 50 kiloton detector. An entry-level machine would permit one to perform a 5σ differentiation of the sign of δm_{32}^2 at a baseline length of ~ 2800 km.

Figure 4 shows the 3σ reach of $\sin^2 2\theta_{13}$ versus baseline length for a 20 GeV muon storage ring (a) with 10^{20} decays, a 50 kiloton detector and positive δm_{32}^2 , (b) for negative δm_{32}^2 for various values of $|\delta m_{32}^2|$. Figures 4 (c) and (d) show the corresponding curves for 10^{19} decays and a 50 kiloton detector. The error bars show the error due to statistical fluctuations in our determination of the 3σ reach. Our results agree with similar calculations in Ref. [14]. It can be seen that an entry-level machine is capable of determining the sign of δm_{32}^2 provided that $\sin^2 2\theta_{13}$ is greater than 0.01 for δm_{32}^2 in the range 0.0025–0.0045 eV².

To conclude, we have shown that the neutrino factory provides a powerful tool to explore the structure of neutrino masses. Even an “entry level” machine with 10^{19} decays of 20 GeV stored muons and a 50 kiloton detector at a baseline exceeding ~ 2800 km is capable of differentiating the sign of δm_{32}^2 for the LAM scenario. The 3σ reach in $\sin^2 2\theta_{13}$ in the sign determination of δm_{32}^2 for such a machine exceeds the present bound on $\sin^2 2\theta_{13}$ by about an order of magnitude.

Acknowledgments

This research was supported in part by the U.S. Department of Energy under Grant No. DE-FG02-95ER40896 and in part by the University of Wisconsin Research Committee with funds granted by the Wisconsin Alumni Research Foundation.

References

- [1] C. Ankenbrandt *et al.*, (Muon Collider Collaboration), Phys. Rev. ST Accel. Beams **2**, 081001 (1999).
- [2] S. Geer, Phys. Rev. **D57**, 6989 (1998).
- [3] R.B. Palmer, C. Johnson, E. Keil, CERN-SL-99-070-AP (1999); J. Ellis, E. Keil, G. Rolandi, “Options for future colliders at CERN”, CERN-EP-98-03, Jan 1998; S. Geer, C. Johnstone, D. Neuffer, “Muon Storage Ring Neutrino Source: The Path to a Muon Collider?”, FERMILAB-TM-2073, March 1999; S. Geer, C. Johnstone, D. Neuffer; “Design concepts for a muon storage ring neutrino source”, FERMILAB-PUB-99-121, April 1999; See http://www.fnal.gov/projects/muon_collider/nu-factory/ for the accelerator feasibility study.
- [4] B. Autin et al., “Physics opportunities at a CERN based neutrino factory”, CERN-SPSC-98-30, Oct. 1998; A. Bueno, M. Campanelli, A. Rubbia, “Long baseline neutrino oscillation disappearance search using a neutrino beam from muon decays”, ETHZ-IPP-PR-98-05, Aug. 1998, hep-ph/9808485; A. Bueno, M. Campanelli, A. Rubbia, “A medium baseline search for $\nu_\mu \rightarrow \nu_e$ oscillations at a neutrino beam from muon decays”, CERN-EP-98-140, Sept. 1998, hep-ph/9809252; B. Autin, A. Blondel, J. Ellis (editors), “Prospective Study of Muon Storage Rings at CERN”, CERN 99-02, April 1999; A. De Rújula, M. B. Gavela, and P. Hernández, Nucl. Phys. **B547**, 21 (1999), hep-ph/9811390; V.Barger, S. Geer, and K. Whisnant, , Phys. Rev. **D 61**, 053004 (2000).

- [5] Super-Kamiokande Collaboration, Y. Fukuda *et al.*, Phys. Lett. **B433**, 9 (1998); Phys. Lett. **B436**, 33 (1998); Phys. Rev. Lett. **81**, 1562 (1998); Phys. Rev. Lett. **82**, 2644 (1999).
- [6] Kamiokande collaboration, K.S. Hirata *et al.*, Phys. Lett. **B280**, 146 (1992); Y. Fukuda *et al.*, Phys. Lett. **B335**, 237 (1994); IMB collaboration, R. Becker-Szendy *et al.*, Nucl. Phys. Proc. Suppl. **38B**, 331 (1995); Soudan-2 collaboration, W.W.M. Allison *et al.*, Phys. Lett. **B391**, 491 (1997); MACRO collaboration, M. Ambrosio *et al.*, Phys. Lett. **B434**, 451 (1998).
- [7] A. de Gouvea, A. Friedland, and H. Murayama, hep-ph/0002064; G.L. Fogli, E. Lisi, D. Mintanino, and A. Palazzo, hep-ph/9912231; M.C. Gonzalez-Garcia, P.C. de Holanda, C. Peña-Garay, and J.W.F. Valle, hep-ph/9906469; M.C. Gonzalez-Garcia and C. Peña-Garay, hep-ph/0002186; J.N. Bahcall, P. Krastev, and A.Yu. Smirnov, Phys. Rev. **D58**, 096016 (1998); hep-ph/9905220; N. Hata and P. Langacker, Phys. Rev. **D56**, 6107 (1997).
- [8] C. Albright *et al.*, “Physics at a Neutrino Factory” FERMILAB-FN-692, April 2000. See the Fermilab Long-Baseline Workshop web site at http://www.fnal.gov/projects/muon_collider/nu/study/study.html
- [9] V. Barger, S. Geer, R. Raja, and K. Whisnant, hep-ph/9911524, Phys. Rev. D (in press); hep-ph/0003184.
- [10] L. Wolfenstein, Phys. Rev. **D17**, 2369 (1978); V. Barger, S. Pakvasa, R.J.N. Phillips, and K. Whisnant, Phys. Rev. **D22**, 2718 (1980); P. Langacker, J.P. Leveille, and J. Sheiman, Phys. Rev. **D 27**, 1228 (1983); S.P. Mikheyev and A. Smirnov, Yad. Fiz. **42**, 1441 (1985) [Sov. J. Nucl. Phys. **42**, 913 (1986)].
- [11] J. Pantaleone, Phys. Rev. **D49**, 2152 (1994); Phys. Rev. Lett. **81**, 5060 (1998).
- [12] M. Campanelli, A. Bueno, and A. Rubbia, hep-ph/9905240.
- [13] I. Mocioiu and R. Shrock, hep-ph/0002149.
- [14] A. Romanino, hep-ph/9909425; M. Freund, M. Lindner, S.T. Petcov, and M. Romanino, hep-ph/9912457; M. Freund, P. Huber, and M. Lindner, hep-ph/0004085.
- [15] R. Bernstein and S. Parke, Phys. Rev. **D44**, 2069 (1991); and M. Lusignoli, Phys. Lett. **B300**, 128 (1993); P. Lipari and M. Lusignoli, Phys. Rev. **D58**, 073005 (1998); E. Akhmedov, A. Dighe, P. Lipari, and A.Yu. Smirnov, Nucl. Phys. **B542**, 3 (1999); E.K. Akhmedov, Nucl. Phys. **B538**, 25 (1998); S.T. Petcov, Phys. Lett. **B434**, 321 (1998); M.V. Chizhov, M. Maris, and S.T. Petcov, hep-ph/9810501; M.V. Chizhov and S.T. Petcov, hep-ph/9903424; S.T. Petcov, hep-ph/9910335; H.W. Zaglauer and K.H. Schwarzer, Z. Phys. **C40**, 273 (1988); Q. Liu, S. Mikheyev, and A.Yu. Smirnov, Phys. Lett. **B440**, 319 (1998); P.I. Krastev, Nuovo Cimento A **103**, 361 (1990); J. Pruet and G.M. Fuller, astro-ph/9904023. J. Arafune, J. Sato, Phys. Rev. **D55**, 1653 (1997); J. Arafune, M. Koike and J. Sato, Phys. Rev. **D56**, 3093 (1997); M. Tanimoto,

- Prog. Theor. Phys. **97**, 901 (1997); H. Minakata and H. Nunokawa, Phys. Lett. **B413**, 369 (1997); H. Minakata and H. Nunokawa, Phys. Rev. **D57**, 4403 (1998); M. Koike and J. Sato, hep-ph/9909469; M. Koike and J. Sato, hep-ph/9911258; T. Ohlsson and H. Snellman, hep-ph/9910546.
- [16] In principle, one can optimize further by running for different periods of time for the different stored charges, to take into account the difference in cross sections for neutrinos and anti-neutrinos in matter, but we have not performed that optimization in this study.
 - [17] Parameters of the Preliminary Reference Earth Model are given by A. Dziewonski, Earth Structure, Global, in “The Encyclopedia of Solid Earth Geophysics”, ed. by D.E. James, (Van Nostrand Reinhold, New York, 1989) p. 331; also see R. Gandhi, C. Quigg, M. Hall Reno, and I. Sarcevic, Astroparticle Physics **5**, 81 (1996).
 - [18] P. Spentzouris, private communication.
 - [19] See R. Raja, Fermilab MUCOOL note MUC/NOTE/PHYSICS/PUBLIC/112 for further details of the fitting procedure.

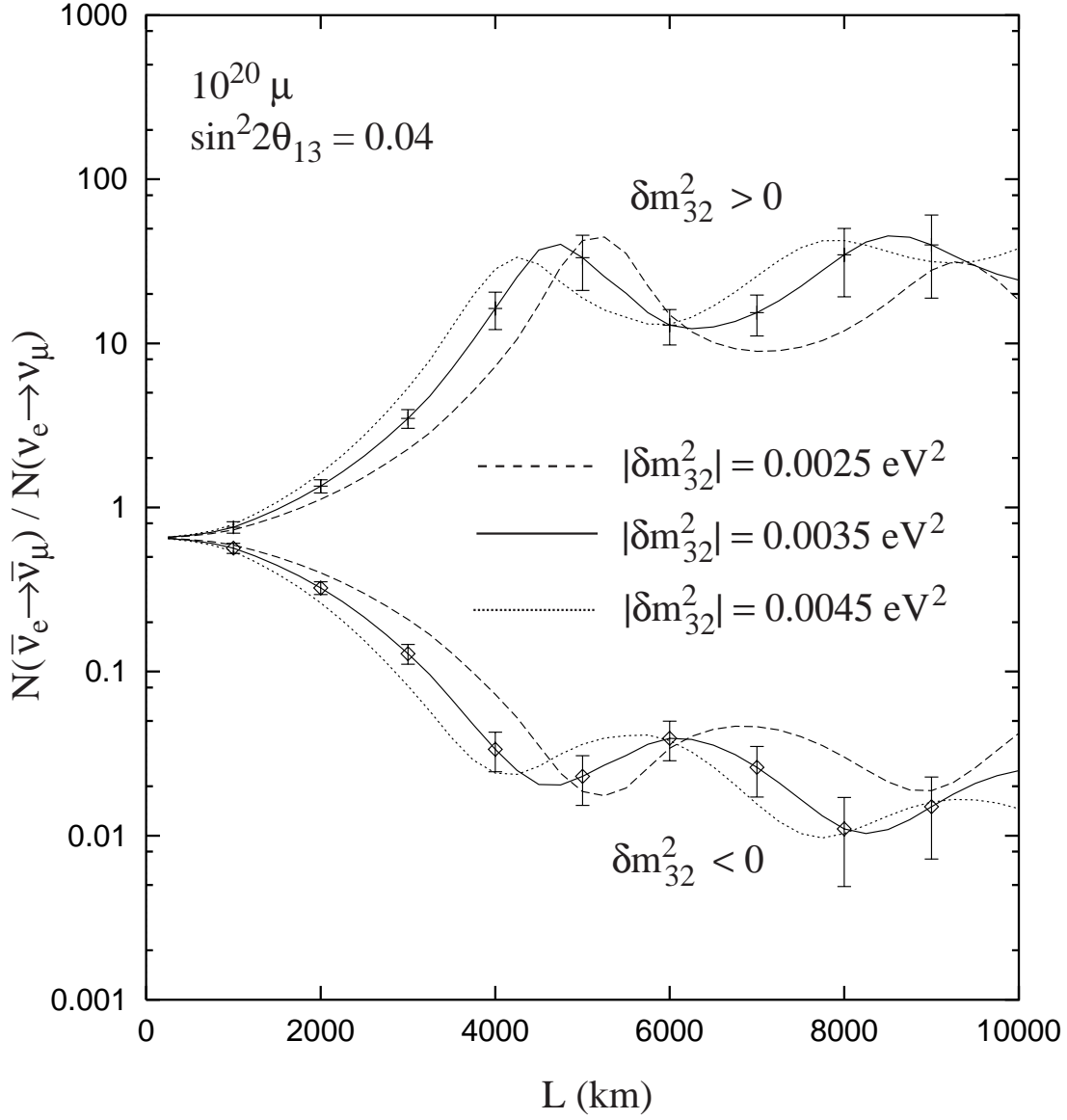


Figure 1: The ratio of wrong-sign muon events $N(\bar{\nu}_e \rightarrow \bar{\nu}_\mu)/N(\nu_e \rightarrow \nu_\mu)$ versus baseline for a 20 GeV muon storage ring for $\delta m_{32}^2 = 0.0025$ eV² (dashed line), 0.0035 eV² (solid line), and 0.0045 eV² (dotted line). The other oscillation parameters are given in Eq. (1). A 4 GeV minimum cut was imposed on the detected muon energy. The error bars are statistical errors with 10^{20} decays and a 50 kiloton detector.

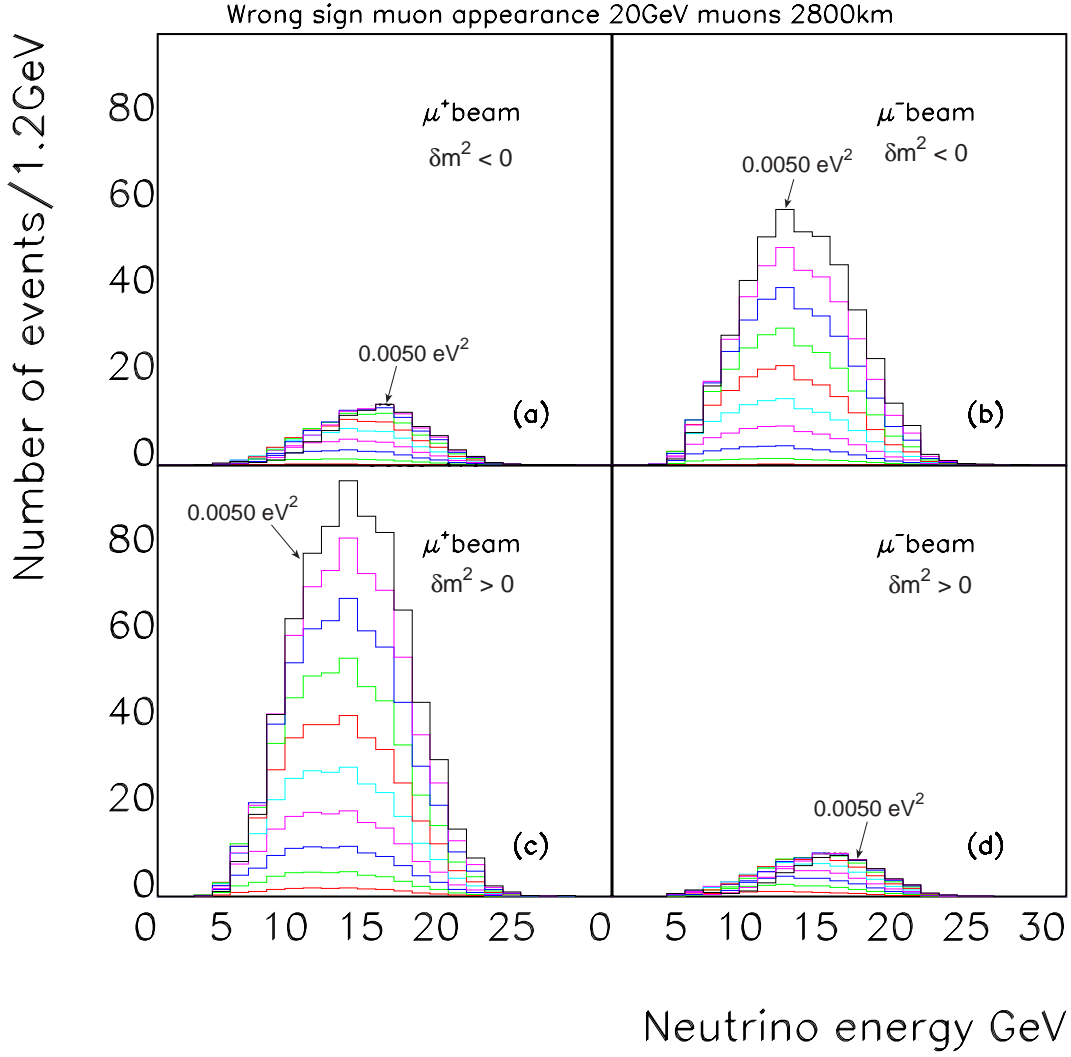


Figure 2: The wrong sign muon appearance rates for a 20 GeV muon storage ring at a baseline of 2800 km with 10^{20} decays and a 50 kiloton detector for (a) μ^+ stored and negative δm_{32}^2 , (b) μ^- stored and negative δm_{32}^2 , (c) μ^+ stored and positive δm_{32}^2 , (d) μ^- stored and positive δm_{32}^2 for values of $|\delta m_{32}^2|$ ranging from 0.0005–0.0050 eV^2 in steps of 0.0005 eV^2 . Matter enhancements are evident in (b) and (c).

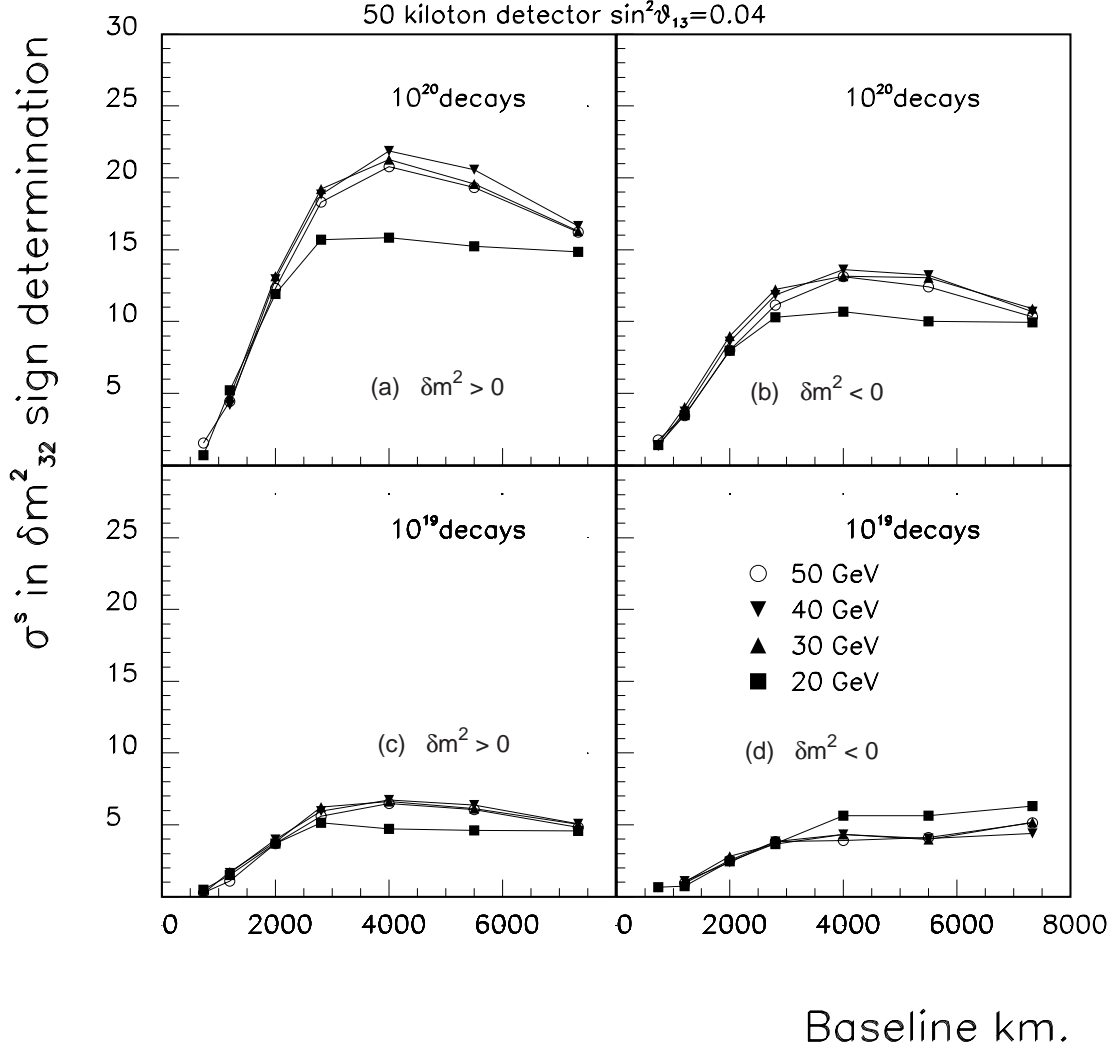


Figure 3: The number of standard deviations to which the sign of δm^2_{32} can be determined versus baseline length for various muon storage ring energies: (a) 50 kiloton detector, 10^{20} μ^+ and μ^- decays and positive values of δm^2_{32} ; (b) 50 kiloton detector, 10^{20} μ^+ and μ^- decays and negative values of δm^2_{32} ; (c) 50 kiloton detector, 10^{19} μ^+ and μ^- decays and positive values of δm^2_{32} ; (d) 50 kiloton detector, 10^{19} μ^+ and μ^- decays and negative values of δm^2_{32} .

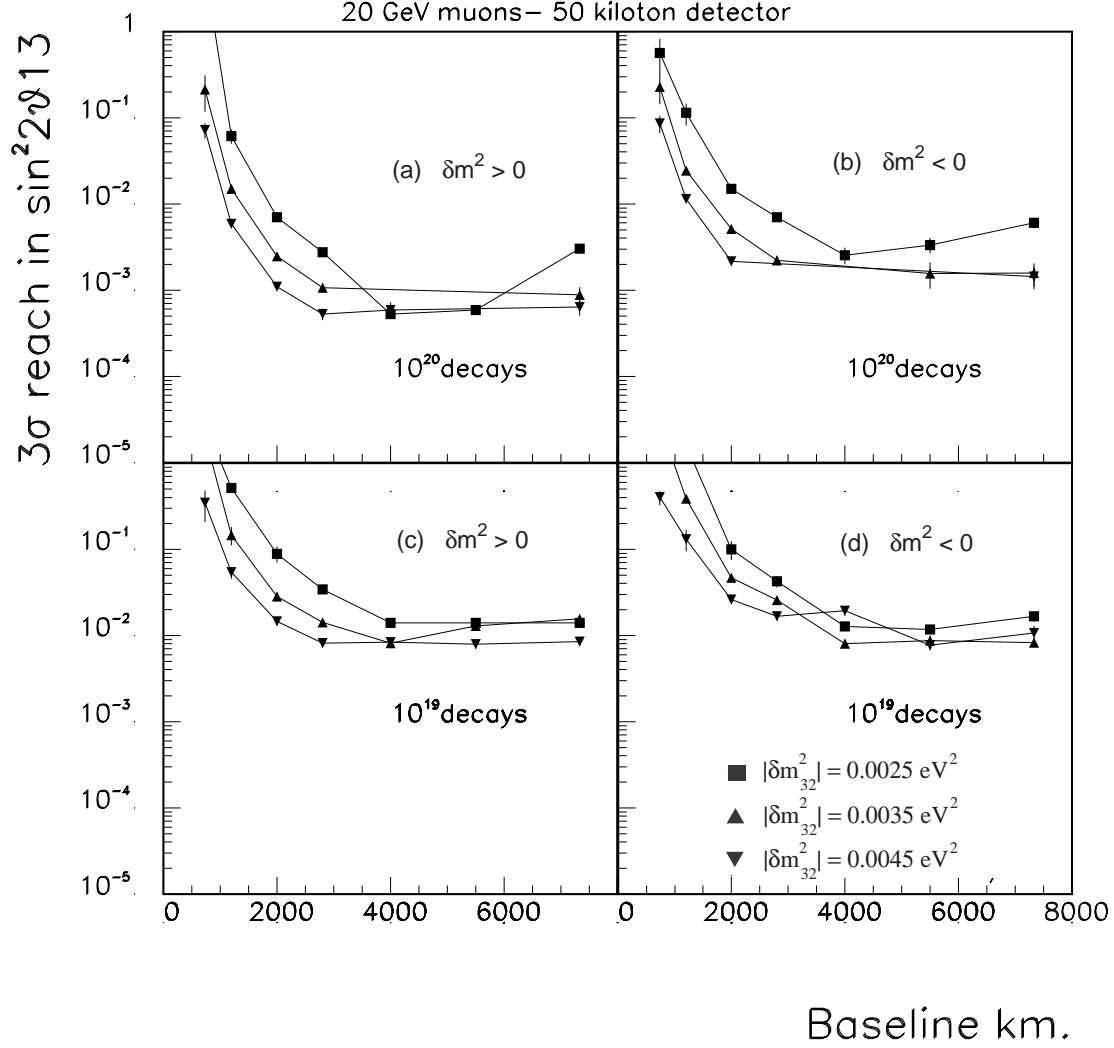


Figure 4: The sensitivity reach in $\sin^2 2\theta_{13}$ at which the sign of δm^2_{32} can be determined to 3 standard deviations versus baseline length for various values of δm^2_{32} : (a) 50 kiloton detector, 10^{20} μ^+ and μ^- decays and positive values of δm^2_{32} ; (b) 50 kiloton detector, 10^{20} μ^+ and μ^- decays and negative values of δm^2_{32} ; (c) 50 kiloton detector, 10^{19} μ^+ and μ^- decays and positive values of δm^2_{32} ; (d) 50 kiloton detector, 10^{19} μ^+ and μ^- decays and negative values of δm^2_{32} .